SIMS ANALYSES OF THE OLDEST KNOWN ASSEMBLAGE OF MICROFOSSILS DOCUMENT THEIR TAXON-CORRELATED CARBON ISOTOPE COMPOSITIONS

J. William Schopf[a,b,c,d,1], Kouki Kitajima[d], Michael J. Spicuzza [d], Anatoliy B. Kudryavtsev[b], John W. Valley[d]

[a]Department of Earth, Planetary, and Space Sciences, University of California, Los Angeles, CA 90095;

[b]Center for the Study of Evolution and the Origin of Life, University of California, Los Angeles, CA 90095;

[c]Molecular Biology Institute, University of California, Los Angeles, CA 90095;

[d]University of Wisconsin Astrobiology Research Consortium, Department of Geoscience, University of Wisconsin, Madison, WI 53706.

Author contributions: J.W.S. and J.W.V. designed research; J.W.S., K.K., M.J.S., A.B.K., and J.W.V. performed research; J.W.S., K.K., M.J.S., and J.W.V. analyzed data; and J.W.S. and J.W.V. wrote the paper.

[1]To whom correspondence may be addressed. Email:
schopf@epss.ucla.edu.

Classification:

PHYSICAL SCIENCES: Earth, Atmospheric, and Planetary Sciences

BIOLOGICAL SCIENCES: Evolution

Short Title

Archaea in the Archean

Key Words

Apex chert; Archaea; Archean; methanogens; methanotrophs

Abstract

Analyses by secondary ion mass spectroscopy (SIMS) of 11 specimens of five taxa of prokaryotic filamentous kerogenous cellular microfossils permineralized in a petrographic thin section of the ~3465 Ma Apex chert of northwestern Western Australia, prepared from the same rock sample from which this earliest known assemblage of cellular fossils was described more than two decades ago, show their $\delta^{13}C$ compositions to vary systematically taxon to taxon from -31‰ to -39‰. These morphospecies-correlated carbon isotope compositions confirm the biogenicity of the Apex fossils and validate their morphology-based taxonomic assignments. Perhaps most significantly, the $\delta^{13}C$ values of each of the five taxa are lower than those of bulk samples of Apex kerogen (-27‰), those of SIMS-measured fossil-associated dispersed particulate kerogen (-27.6‰), and those typical of modern prokaryotic phototrophs (-25 ±10‰). The SIMS data for the two highest $\delta^{13}C$ Apex taxa are consistent with those of extant phototrophic bacteria; those for a somewhat lower $\delta^{13}C$ taxon, with non-bacterial methane-producing Archaea; and those for the two lowest $\delta^{13}C$ taxa, with methane-metabolizing γ-Proteobacteria. Although the existence both of methanogens and methanotrophs has been inferred from bulk analyses of the carbon isotopic compositions of pre-2500 Ma kerogens, these *in situ* SIMS-analyses of individual microfossils present the first data interpretable as evidencing the cellular

preservation of such microorganisms and are consistent with the near-basal position of the Archaea in rRNA phylogenies.

Significance Statement

Although the existence of the Archaea (one of three all-encompassing Domains of Life) in the Archean Eon (4000 to 2500 million years ago) has been inferred from carbon isotopes in bulk samples of ancient rocks, their cellular fossils have been unknown. We here present carbon isotope analyses of 11 microbial fossils from the ~3465 million-year-old Western Australian Apex chert from which we infer that two of the five species studied were primitive photosynthesizers, one an Archaeal methane-producer, and two others methane-consumers. This discovery of Archaea in the Archean is consistent with the rRNA "Tree of Life," confirms the earlier disputed biogenicity of the Apex fossils and suggests that methane-cycling methanogen-methanotroph communities were a significant component of Earth's early biosphere.

\body

Widely regarded as among the oldest known evidence of life, the morphologically diverse cellular carbonaceous (kerogenous) microscopic fossils of the ~3465 Ma Apex chert, systematically described more than two decades ago (1, 2), have been a focus of controversy. Perhaps spurred by a reluctance to affirm the veracity of "claims for life in the earliest 2.0-2.5 billion years of Earth's history" (3), some workers have suggested the Apex fossils to be chert-embedded mineralic pseudofossils composed of "abiotic graphite" (4, 5), barium carbonate (6, 7), or hematite in secondary veinlets (8). Other studies implied that the fossils are non-indigenous clay mineral needle-like crystallites (9) or suggested them to be composed of "vermiculate-like" minerals produced via a "nonbiological formation model" involving the hydration and exfoliation of mica flakes followed by their surficial adsorption of later-introduced hydrocarbons (10).

Principal deficiencies of these suggestions are that carbonaceous (kerogenous) cellular microbe-like assemblages of nonbiologic pseudofossils are evidently unknown in the geological record; abiologically produced kerogenous particulate organic matter is similarly unreported from the geological record; and virtually none of these studies is reported to have been based on examination of the scores of demonstrably kerogenous (4, 11, 12) morphometrically diverse well-

96 characterized (1, 2) originally described Apex specimens archived at London's
97 Natural History Museum (NHM; ref. 2).

98 Although the earlier disputed biogenicity of the Apex fossils seems largely to
99 have been laid to rest (12), the biological affinities and physiological
100 characteristics of these exceedingly ancient fossil microbes remain to be
101 established. Initially formally described as "prokaryotes *Incertae Sedis*" – non-
102 nucleated microorganisms of uncertain and undefined systematic relations (ref. 2,
103 p. 643) – the present study suggests a solution to this unresolved problem.

104 We here present results of *in situ* analyses of 11 specimens of five taxa of
105 permineralized microscopic fossils embedded in Apex chert petrographic thin
106 section 4 of 6/15/82-1H prepared from the same rock sample at the same time as
107 the six holotype- and paratype-containing sections previously archived at the NHM
108 (sections 4 of 6/15/82-1B through -1G; refs 1, 2). The indigenousness and
109 syngenicity of the permineralized fossils to their encompassing chert matrix is
110 shown by optical microscopy supported by Raman spectroscopy which also
111 establishes their kerogenous composition. The biogenicity and taxonomic relations
112 of the analyzed fossils are documented by their demonstrably cellular cylindrical
113 filamentous morphology; the taxon-defining size-ranges of their medial cells and,
114 where preserved, the morphology of their terminal cells; and their morphometric
115 comparison to previously reported specimens from the same rock. Analyses of

each of the 11 specimens by secondary ion mass spectroscopy (SIMS) document the carbon isotope compositions of the five taxa studied.

The taxon-correlated SIMS carbon-isotope data reported here reaffirm the carbonaceous, kerogenous (rather than mineralic) composition of the exceedingly ancient Apex fossils; reinforce the widely assumed (but difficult to firmly establish) validity of the use of cellular and organismal morphology for the assignment of ancient microbes to biologically meaningful taxonomic categories; and provide insight into the physiology and biological affinities of the five Apex taxa examined.

Results and Discussion

Geologic Setting. Geologically initially mapped as a shallow marine facies (13, 14), the fossiliferous locality (3) of the ~3465 Ma Apex chert (15) has more recently been reinterpreted to be a brecciated and altered hydrothermal vein deposit (16). The 11 specimens of five taxa of permineralized microscopic fossils analyzed here are embedded in Apex chert petrographic thin section 4 of 6/15/82-1H prepared from a rock sample collected from outcrop in 1982 (cf. refs. 1, 2).

Although a hydrothermal environment has been suggested to be unlikely for preservation of delicate fossil microbes (4, 5, 9), biota-prohibiting hydrothermal temperatures for the genesis of the Apex chert have not been demonstrated; microorganisms morphologically comparable to the Apex filaments are common in modern hydrothermal settings (17); filamentous microbes similar to *Primaevifilum amoenum*, the most abundant of the described Apex taxa (2), have long been known to occur at deep-sea thermal vents (18); and chert-permineralized fossil filaments, including specimens so similar to those of the Apex chert that they have been assigned to two of the Apex taxa (19), are present in three other Paleoarchean hydrothermal units of the northwestern Australian Pilbara Craton (19-24).

Specimens Analyzed. The locations of the 11 SIMS-analyzed Apex microfossils in chert thin section 4 of 6/15/82-1H are shown in Fig. 1a-n compared with three previously described Apex specimens (Fig. 1p-z) permineralized in NHM-archived thin section 4 of 6/15/82-1B (ref. 2).

As is shown (Fig. 1a, e, h, o), the Apex fossils typically occur in subrounded millimeter-sized carbonaceous chert clasts in which they are embedded in flocculent organic matter. Within such clasts the Apex fossils are commonly rather closely spaced, numerous specimens occurring within a given granular clast (Fig. 1h-n, p-s). Optical photomicrographs (e.g., Fig. 1d, q-s) and three-dimensional

(Fig. 1t) and two-dimensional (Fig. 1u-z) Raman images of the fossils show them to be cellular, exhibiting box-like cell lumina-enclosing kerogenous cell walls.

Like some of the microfossils permineralized in other Paleoarchean hydrothermal units, it is possible that the Apex filaments represent remnants of thermophilic microbes preserved *in situ*. Given their clast-embedded mode of occurrence, however, it seems more likely that the fossils are allocthonous to the deposit, older than or penecontemporaneous with the Apex chert, fossilized microbes emplaced in the unit in reworked detrital carbonaceous granules.

Data documenting the carbonaceous (kerogenous) composition of each of the 11 SIMS-analyzed Apex specimens are shown in Figure 2, two-dimensional Raman images acquired at the kerogen "G" band (~1605 cm^{-1}) accompanied by optical photomicrographs of the specimens studied. Such data, acquired routinely to differentiate *bona fide* microfossils from mineralic "fossil-like" microscopic objects, provided the biogenic targets for subsequent SIMS analyses.

Figure 3 and Dataset S1 present pre- and post-SIMS images of the Apex fossils discussed here showing that the SIMS-analyzed pits spatially correspond to the specimens exposed at the surface of the polished thin section. Table 1 summarizes the SIMS-measured $\delta^{13}C$ values of the 11 specimens of the five taxa analyzed. Details regarding SIMS analyses of these specimens, measurements that

174 we regard as among the most reliable reported for microfossils in chert, are
175 documented in the *Supplementary Information.*
176
177 **Biological Affinities of the Apex Fossils.** SIMS $\delta^{13}C$ data for the 11 Apex fossils
178 analyzed (Figs.1-3; Table 1) provide a means to assess the physiology and
179 biological affinities of the five taxa studied. The $\delta^{13}C$ values of the individual
180 fossils reported here range from -29.8‰ to -44.1‰ (Table 1), the data showing
181 that each of the five morphometrically defined taxa has a characteristic carbon-
182 isotope composition that varies taxon to taxon from the highest in $\delta^{13}C$ (an
183 unnamed unicell, -30.9‰ , and *Primaevifilum minutum*, -31.6‰) to the lowest
184 (*Archaeocillatoriopsis disciformis*,-39.2‰ and *P. amoenum*, -39.4‰). The SIMS-
185 determined $\delta^{13}C$ values of the fossils thus differ from those of bulk samples of
186 Apex kerogen (-27‰; ref. 25) and those of SIMS measurements acquired away
187 from the fossils to determine the $\delta^{13}C$ values of particulate kerogen dispersed in the
188 chert matrix (~-27.6‰; Dataset S2, Table S1).
189 As discussed below, the microfossil $\delta^{13}C$ values are similar to those of extant
190 prokaryotic phototrophs, methanogenic Archaeans, and γ-Proteobacterial
191 methanotrophs.
192 Direct evidence of the biological affinities of the Apex fossils is limited to
193 their (1) cellular and organismal morphologies and (2) SIMS-measured carbon-

194 isotope ratios, the plausibility of the resulting interpretations being evaluated by (3)
195 the similarity of their morphologies and $\delta^{13}C$ values to extant microorganisms and
196 their consonance with inferences based on (4) available geochemical and fossil
197 data from comparably ancient sediments and (5) the position of the inferred
198 biological lineages on the phylogenic rRNA "Tree of Life." As noted above for
199 these evidently allocthonous clast-embedded specimens (Fig. 1), a sixth typically
200 relevant criterion, their original ecological setting, cannot currently be accurately
201 assessed.

202 Below we evaluate the biological affinities of the Apex taxa in three
203 categories ordered by their SIMS-determined highest to lowest average $\delta^{13}C$ values
204 (Table 1).

205 (1) Unnamed unicell, $\delta^{13}C$ -30.9‰ (Figs. 1n, 2u, v, 3i, j) and *Primaevifilum*
206 *minutum*, $\delta^{13}C$ -31.6‰ (Figs. 1f, g, k, 2o-t, 3e, f, s-v). Extant prokaryotic
207 phototrophs have $\delta^{13}C$ values reported to range for cyanobacteria from -8‰ to -
208 31‰, and for non-oxygenic photosynthetic bacteria from -19‰ to -36‰ (26). The
209 ranges of $\delta^{13}C$ values of the three analyzed specimens of the unnamed unicell and
210 *P. minutum* overlap with the $\delta^{13}C$ values of such extant phototrophs, their
211 morphologies also being similar to those of diverse modern (27) and Precambrian
212 mat-building (stromatolitic) microbial phototrophs, both Archean (e.g., 24, 28) and

Paleoproterozoic (e.g., 29), in which, as we infer for the organic-rich clasts of the Apex chert, microbes of diverse physiologies co-occur on a millimetric scale.

(2) *P. delicatulum,* $\delta^{13}C$ -35.4‰ (Figs. 1i-m, 2k-n, 3e-h, k-n). Although the average $\delta^{13}C$ value of the four specimens of this taxon analyzed marginally overlaps with the lowest values recorded for extant anoxygenic phototrophs (-36‰; ref. 26), their range of carbon isotope values (32.7 to -38.2‰; Table 1) is particularly similar to that of modern methanogenic Archaeans (-27‰ to -38‰; ref. 26). Nevertheless, the cellular 1.8 to 3.2µm-broad filaments of *P. delicatulum* (2) differ markedly in morphology from described methanogens, almost all such modern taxa being composed of spherical, rod-shaped, or rectangular single cells. The sole filamentous methanogen yet reported, *Thermofilum*, is characterized by thin straight or curved filaments 0.1 to 0.3µm broad (30, 31) and, thus, is unlike the much broader filaments of the Apex taxon. This apparent absence of a modern morphological analogue of *P. delicatulum* may reflect the relatively recent, 1990 recognition of the Archaea Domain (32) and a resulting lack of comprehensive surveys of extant members of the group or, perhaps, the possibility that the ~3465 Ma Apex taxon represents an early-evolved but now extinct Archaeal lineage.

(3) *Archaeocillatoriopsis disciformis*, $\delta^{13}C$ -39.2‰ (Figs. 1b, c, 2a-d, 3 k-p) and *P. amoenum,* $\delta^{13}C$ -39.4‰ (Figs. 1d, 2i j, 3, q, r). Relative to extant prokaryotic phototrophs and methanogens, the SIMS-measured carbon isotope

values of the three specimens comprising this grouping are appreciably lower. Characteristically low $\delta^{13}C$ Archaeal methanogen-produced methane, having values of -50 to -110‰ (33), is a logical candidate for the source of such carbon, a supposition used to explain the occurrence both of the comparably low $\delta^{13}C$ values of carbonaceous matter in pre-2500 Ma sediments (34, 35) and modern microbial communities in which, as we infer for the Apex assemblage, anaerobic methane-producers and -consumers intimately coexist (e.g., 33, 36).

Incorporation of low $\delta^{13}C$ methane into potentially fossilizable biomass is carried out by γ-Proteobacterial methanotrophs, members of the largest class of the gram-negative Proteobacteria (37) among which they are unique by using methane as their sole carbon and energy source (38). However, virtually all such methanotrophs are small single-celled rods, coccoids or ellipsoids (38, 39) that differ distinctly in cellular morphology from much larger-diameter filamentous specimens of *A. disciformis* and *P. amoenum*. The single exception to this generalization known to us is *Crenothrix polyspora* Cohn 1870, a filamentous bacterium now studied for 150 years (27, 40-42) but only recently shown to be a γ-Proteobacterial methanotroph (43, 44), a modern taxon characterized as unbranched filaments composed of cylindrical to disc-shaped cells ~1- to ~6μm broad (27) and thus similar to the 1.8 to 5μm-diameter quadrate to disc-shaped cell-containing filaments of *A. disciformis* and *P. amoenum* (2).

253 Regardless of whether *C. polyspora* represents a modern analogue of
254 Paleoarchean *A. disciformis* and/or *P. amoenum* – at present there being
255 insufficient data to establish such relationships – the low $\delta^{13}C$ SIMS-documented
256 compositions of these ~3465 Ma fossil taxa are most plausibly interpreted as
257 evidencing methanotrophy. This, in turn, requires the presence of biogenic
258 methane produced by Archaeal methanogens, inferred from the SIMS-data to have
259 perhaps been generated by taxa such as *P. delicatulum*. Although the SIMS data
260 do not exclude the possible affinity of two of the Apex taxa (an unnamed unicell
261 and *P. minutum*) to phototrophic cyanobacteria and/or photosynthetic bacteria,
262 those of three of the taxa are more plausibly interpreted as evidencing an early-
263 evolved methanogen-methanotroph biocoenose, physiological characteristics
264 compatible with the near-basal position of methane-generating Archaea in rRNA
265 phylogenies (32).
266 Such fossils would comprise the first cellularly preserved members of the
267 Archaea Domain and γ-Proteobacterial methanotrophs identified in the geological
268 record and, given the obligate anaerobic metabolism of methane-producing
269 Archaea and the oxygen-deficient setting inhabited by extant methanogen-
270 methanotroph communities (33, 36), consonant also with an anoxic early
271 environment (45, 46).
272

Conclusions

From the data summarized above (and presented in the *Supplementary Information*) we interpret these SIMS-based carbon-isotope analyses of 11 specimens of five taxa of the ~3465 Ma Apex chert of northwestern Western Australia to indicate that:

(1) Their taxon-correlated SIMS $\delta^{13}C$ values reinforce both their biogenicity and the widely held assumptions that the organismal and cellular morphology of ancient microbes can be used to establish biologically meaningful taxonomic categories and provide insight into the physiology and biological affinities of the specimens analyzed.

(2) Two of the taxa exhibit $\delta^{13}C$ compositions not inconsistent with phototrophic metabolism.

(3) SIMS data for the other three Apex taxa studied are more compatible with affinities to Archaeal methanogens and γ-Proteobacterial methanotrophs, physiological characteristics consonant with the near-basal position of the Archaea in rRNA phylogenies.

(4) These fossils may therefore comprise the first cellularly preserved members of the Archaea Domain and of γ-Proteobacterial methanotrophs to be identified in the geological record, their preservation in this ~3465 Ma deposit

suggesting that methane-cycling methanogen-methanotroph communities were a significant component of the Paleoarchean biosphere.

Materials and Methods

Optical Microscopy. Optical images of the thin section-embedded specimens studied here were acquired at the University of California, Los Angeles (UCLA) using fluorescence-free microscopy immersion oil and a Leitz Orthoplan 2 microscope equipped with a Nikon DS Microscope Digital Camera.

Raman Spectroscopy. Molecular-structural compositional analyses of the fossils were carried out at UCLA using a T64000 triple-stage confocal laser-Raman system that permits acquisition both of point spectra and of Raman images that display the two-dimensional spatial distribution of the molecular-structural components of the specimens and their associated minerals, images that can be stacked to provide a three-dimensional image of the specimens analyzed. A Coherent Innova argon ion laser provided excitation at 457.9 nm permitting data to be obtained over a range from ~300 to ~3000 cm^{-1} using a single spectral window centered at 1800 cm^{-1}. The laser power used was ~6-8 mW over a ~1 μm spot, a

313 configuration well below the threshold resulting in radiation damage to kerogenous
314 fossils, and the thin sections were covered by a veneer of fluorescence-free
315 microscopy immersion oil, the presence of which has no discernable effect on the
316 Raman spectra acquired. Varying pixel intensities in the acquired two-dimensional
317 Raman images correspond to the relative concentrations of the material analyzed.
318
319 **Secondary Ion Mass Spectrometry (SIMS).** At the University of Wisconsin-
320 Madison WiscSIMS Laboratory, analyses of the carbon isotope compositions of
321 the optically and Raman-identified micron-sized permineralized fossils in
322 petrographic thin section 4 of 6/15/82-1H were carried using a SIMS CAMECA
323 IMS 1280. Fossil-containing areas were excised by use of a water-cooled diamond
324 saw; cleaned in ethanol; mounted in epoxy together with two grains of the Bolton
325 scapolite standard (Bolt, Me_{69}; ref. 47); and ground and polished using a water-
326 lubricated diamond paste to expose the target fossils at their surface. Calibration
327 of $\delta^{13}C$ was performed using a separate 25-mm-diameter epoxy-mount containing
328 the Bolt standard and carbon isotope standard PPRG215 (48, 49). Two types of
329 PPRG215 mounts were used, grain- and chip-mounts (Figs. S1, S2). The Bolt
330 standard was calibrated based on PPRG215 and analyzed as a running standard.
331 All mounts were cleaned with ethanol and gold-coated prior to analyses.

SIMS-data were collected in two analytical sessions (Session-1, 5/9/2016-5/12/2016; and Session-2, 5/1/2017-5/2/2017). Following analysis of each specimen, SIMS pits were imaged by scanning electron microscopy (SEM) and the epoxy mounts were reground and re-polished to expose new target fossils at their surface (Supplementary Figures-2). After subsequent re-polishing and before SIMS-analyses, the newly exposed specimens were imaged by optical microscope and SEM.

Analyses of carbon isotope ratios were acquired using a $^{133}Cs^{+}$ primary ion beam typically having a ~12-μm-diameter spot size, an intensity of 2.7-2.9 nA, and a secondary ion accelerating voltage of 10 kV. Details of the analytical conditions used are described by Morag et al. (48). Measurements of the carbon standard mount (Bolt and PPRG215) were performed using the same analytical conditions. To assure the reliability of the results obtained, during the course of the two analytical sessions the carbon-isotope standard was analyzed 190 times (130 spots in Session-1, 60 in Session-2; Figs. S3-5).

For use of this 12-μm-diameter spot size, external precision was 1.3-2.6‰ (2 SD, including the calculated uncertainties of the running and calibration standards, and internal errors). Some of the specimens analyzed contained low concentrations of carbon that yielded low secondary-ion count rates having poor analytical precision (see Figs. S6, S7 and Dataset S1). Because the concentration

of carbon in the microfossils and that in the chert matrix measured at a distance from the fossils (Fig. 3) was variable, two cut-offs were applied to the acquired data based on the secondary ion ^{12}C count rate: relatively C-rich values, >8.6 Mcps (>3 Mcps/nA), were accepted, whereas values between 8.6 and 4.3 Mcps (3 to 1.5 Mcps/nA) were regarded as marginally acceptable. Values less than 4.3 Mcps were regarded as unreliable. Cut-off values were determined by the average count rate of 130 randomly selected spots on carbon standard PPRG215 in two different mounts during analytical Session-1.

Repository of SIMS-Analyzed Specimens

The specimens here analyzed have been archived by J. W. Valley in the collections of the Geology Museum of the Department of Geoscience, University of Wisconsin, Madison, WI.

ACKNOWLEDGEMENTS. This paper is dedicated to John M. Hayes who 35 years ago (34) was first to postulate that the low $\delta^{13}C$ values of some Archean kerogens evidence the metabolic consumption of Archaeal-produced methane by γ-Proteobacterial methanotrophs like those here inferred to have been present in the Apex microbial assemblage. We thank Chris House (Penn State University) for providing a sample of carbon isotope standard PPRG215, obtained from the

372 Schopf-curated Precambrian Paleobiology Research Group collections at UCLA;
373 and, at the University of Wisconsin, Brian Hess for skillful attention to the
374 repeated and delicate grinding and polishing required to expose the Apex
375 microfossils at the section-surface for SIMS analysis; and Ken Williford (now on
376 the staff of NASA's Jet Propulsion Laboratory, Pasadena, CA) and Navot Morag
377 (now at the University of Jerusalem) for assistance in development of the SIMS
378 $\delta^{13}C$ standard and of protocols for analyses of kerogens. This research was
379 supported by the NASA Astrobiology Institute and the Center for the Study of
380 Evolution and the Origin of Life at UCLA. WiscSIMS is supported by NSF (EAR-
381 1355590) and UW-Madison.

382

383

384 **References**

385

386 1. Schopf JW (1992) Paleobiology of the Archean. *The Proterozoic Biosphere, A*
387 *Multidisciplinary Study*, eds Schopf JW, Klein C (Cambridge University Press,
388 New York), pp. 25-39.
389 2. Schopf JW (1993) Microfossils of the Early Archean Apex chert: new evidence
390 of the antiquity of life. *Science* 260: 640-646.
391 3. Moorbath S (2005) Palaeobiology: dating earliest life. *Nature* 434: 155.

392 4. Brasier MD et al. (2002) Questioning the evidence of Earth's oldest fossils.
393 *Nature* 416: 76-81.
394 5. Brasier MD et al. (2005) Critical testing of Earth's oldest putative fossil
395 assemblage from the ~3.5 Ga Apex chert, Chinaman Creek, Western Australia.
396 *Precam Res* 140: 55-102.
397 6. García-Ruíz JM, Carnerup A, Christy AG, Welham NJ, Hyde ST (2002)
398 Morphology: an ambiguous indicator of biogenicity. *Astrobiology* 2: 353-369.
399 7. García-Ruiz JM, Hyde ST, Carnerup AM, Christy AG, Van Kranendonk MJ,
400 Welham NJ (2003) Self-assembled silica-carbonate structures and detection of
401 ancient microfossils. *Science* 302: 1194-1197.
402 8. Marshall CP, Emry JR, Marshall AO (2011) Haematite pseudomicrofossils
403 present in the 3.5-billion-year-old Apex chert. *Nature Geosci* 4: 240-243.
404 9. Pinti DL, Mineau R, Clement, V (2009). Hydrothermal alteration and
405 microfossil artefacts of the 3,465-million-year-old Apex chert. *Nature Geosci* 2:
406 640-643.
407 10. Brasier M, Antcliffe J, Saunders M, Wacey D (2015) Changing the picture of
408 Earth's earliest fossils (3.5-1.9 Ga) with new approaches and new discoveries.
409 *Proc Natl Acad Sci USA* 112: 4859-4864.
410 11. Schopf JW, Kudryavtsev AB, Agresti DG, Wdowiak T, Czaja AD (2002)
411 Laser-Raman imagery of Earth's earliest fossils. *Nature* 416: 73-76.

412 12. Schopf JW, Kudryavtsev AB (2012) Biogenicity of Earth's earliest fossils: a
413 resolution of the controversy. *Gondwana Res* 22: 761-771.
414 13. Hickman AH, Lipple SL (1978) *Explanatory Notes, Marble Bar 1:250,000*
415 *Geological Map Series 24* (Geological Survey of Western Australia, Perth,
416 Australia).
417 14. Hickman AH (1983) Geology of the Pilbara block and its environs. *Geol Surv*
418 *W Aust Bull* 127: 1-268.
419 15. Hickman AH (2012) Review of the Pilbara Craton and Fortescue Basin,
420 Western Australia: Crustal evolution providing environments for early life. *Island*
421 *Arc* 21: 1-31
422 16. Van Kranendonk MJ (2006) Volcanic degassing, hydrothermal circulation and
423 the flourishing of early life on Earth: a review of the evidence from c. 3490–3240
424 Ma rocks of the Pilbara Supergroup, Pilbara Craton, Western Australia. *Earth-Sci*
425 *Rev* 74: 197-240.
426 17. Pentecost A (2003) Cyanobacteria associated with hot spring travertines. *Can J*
427 *Earth Sci* 40: 1447-1457.
428 18. Jannasch HW, Wirsen CO (1981) Morphological survey of microbial mats near
429 deep-sea thermal vents. *Appl Environ Microbiol* 41: 528-538.
430 19. Ueno Y, Yoshioka H, Isozaki Y (2004**)** Carbon isotopes and petrography in
431 ~3.5 Ga hydrothermal silica dykes in the North Pole area, Western Australia.

Geochim Cosmochim Acta 68: 573-589.

20. Rasmussen B (2000) Filamentous microfossils in a 3235-million-year-old volcanogenic massive sulphide deposit. *Nature* 405: 676-679.

21. Ueno Y, Isozaki Y, Yurimoto H, Maruyama S (2001a) Carbon isotopic signatures of individual Archean microfossils(?) from Western Australia. *International Geological Review* 43, 196-212.

22. Ueno Y, Maruyama, S, Isozaki, Y, Yurimoto, H (2001b) Early Archaean (ca. 3.5 Ga) microfossils and ^{13}C depleted carbonaceous matter in the North Pole area, Western Australia: field occurrence and geochemistry. *Geochemistry and the Origin of Life*, eds Nakashima S, Maruyama S, Brack A, Windley BF (Universal Academic Press, New York), pp. 203-236.

23. Kiyokawa S, Ito T, Ikehara M, Kitajima F (2006) Middle Archean volcano-hydrothermal sequence: bacterial microfossil-bearing 3.2-Ga Dixon Island Formation, coastal Pilbara terrain, Australia. *Geol Soc Am Bull* 118: 3-22.

24. Schopf JW (2006) Fossil evidence of Archaean life. *Phil Trans Roy Soc B: Biol Sci* 61: 869-885.

25. Strauss H, Moore TB (1992) Abundances and isotopic compositions of carbon and sulfur species in whole rock and kerogen samples *The Proterozoic Biosphere, A Multidisciplinary Study*, eds Schopf JW, Klein C (Cambridge University Press, New York), pp. 709-798.

452 26. Schidlowski M, Hayes JM, Kaplan IR (1983) Isotopic inferences of ancient
453 biochemistries: carbon, sulfur, hydrogen, and nitrogen. *Earth's Earliest Biosphere:*
454 *Its Origin and Evolution*, ed Schopf JW (Princeton University Press, New York),
455 pp. 149-186.
456 27. Buchannan RE, Gibbons NE (1975) *Bergey's Manual of Determinative*
457 *Bacteriology, 8th Ed* (Williams Wilkins, Baltimore MD), 1268 pp.
458 28. Schopf JW, Walter MR (1983) Archean microfossils: new evidence of ancient
459 microbes. *Earth's Earliest Biosphere: Its Origin and Evolution*, ed Schopf JW
460 (Princeton University Press, New York), pp. 214-239.
461 29. Hofmann HJ, Schopf JW (1983) Early Proterozoic microfossils. *Earth's*
462 *Earliest Biosphere: Its Origin and Evolution*, ed Schopf JW (Princeton University
463 Press, New York), pp. 321-360.
464 30. Burggraf S, Huber H, Stetter KO (1997) Reclassification of the Crenarchaeal
465 orders and families in accordance with 16s rRNA sequence data. *Internat J Syst*
466 *Bacteriol* 47: 657-660.
467 31. Toshchakov SV et al. (2015) Complete genome sequence of and proposal of
468 *Thermofilum uzonense* sp. nov. a novel hyperthermophilic crenarchaeon and
469 emended description of the genus *Thermofilum*. *Stand Genom Sci* 10: 122-130.

32. Woese CR, Kandler O, Wheelis M (1990) Towards a natural system of organisms: proposal for the domains Archaea, Bacteria, and Eucarya. *Proc Natl Acad Sci USA* 114: 4576-4579.

33. Alperin MJ, Hoehler TM (2009) Anaerobic methane oxidation by Archaea/sulfate-reducing bacteria aggregates: 2. Isotopic constraints. *Am J Sci* 309: 958-984.

34. Hayes JM (1983) Geochemical evidence bearing on the origin of aerobiosis: a speculative hypothesis. *Earth's Earliest Biosphere: Its Origin and Evolution*, ed Schopf JW (Princeton University Press, New York), pp. 291-301.

35. Hayes JM (1993) Factors controlling ^{13}C contents of sedimentary organic compounds: principles and evidence. *Mar Geol* 113: 111-125.

36. Ding H, Valentine DL (2008) Methanotrophic bacteria occupy benthic microbial mats in shallow marine hydrocarbon seeps, Coal Oil Point, California. *J Geophys Res* 113. doi:10.1029/2007JG000537, 2008.

37. Woese CR (1987) Bacterial evolution. *Microbiol Rev* 51: 221-271.

38. Hanson RS, Hanson TE (1996) Methanotrophic bacteria. *Microbiol Rev* 60: 439-471.

39. Whittenbury R, Phillips KC, Wilkinson JF (1970) Enrichment, isolation and some properties of methane-utilizing bacteria. *J Gen Microbiol* 61: 205-218.

40. Cohn F (1870) Uber den Brunnenfaden (*Crenothrix polyspora*) mit Bemerkungen fiber die mikroskopische Analyse des Brunnenwassers. *Beitr Biol Pflanz* 1: 108–131.

41. Harder E (1919) Iron-depositing bacteria and their geologic relations. *US Geol Surv Prof Pap 113* (U.S. Geological Survey, Washington, DC)

42. Kolk LA (1938) A comparison of the filamentous iron organisms, *Clonothrix fusca* Roze and *Crenothrix polyspora* Cohn. *Am J Bot* 25: 11–17.

43. Stoecker K et al. (2006) Cohn's *Crenothrix* is a filamentous methane oxidizer with an unusual methane monooxygenase. *Proc Natl Acad Sci USA* 103: 2363-2367.

44. Vigliotta G et al. (2007) *Clonothrix fusca* Roze 1896, a filamentous, sheathed, methanotrophic γ-proteobacterium. *Appl Environ Microbiol* 73: 3556-3565.

45. Schopf, JW et al. (2017) An anaerobic ~3400 Ma shallow-water microbial consortium: presumptive evidence of Earth's Paleoarchean anoxic atmosphere. *Precam Res* 299: 309-318.

46. J. Farquhar, Bao H, Thiemens JMH (2000) Atmospheric influence of Earth's earliest sulfur cycle. *Science* 289: 756-758.

47. Moecher DP, Valley JW, Essene EJ (1994) Extraction and Carbon Isotope Analysis of CO_2 from Scapolite in Deep Crustal Granulites and Xenoliths. *Geochim Cosmochim Acta* 58: 959-967.

509 48. Morag N, et al. (2016) Microstructure-specific carbon isotopic signatures of
510 organic matter from ~3.5 Ga cherts of the Pilbara Craton support a biologic origin.
511 *Precam Res* 275: 429–449.
512 49. Williford KH, et al. (2013) Preservation and detection of microstructural and
513 taxonomic correlations in the carbon isotopic compositions of individual
514 Precambrian microfossils, *Geochim Cosmochim Acta* 104: 165-182.

515

516

517 **Figure Legends**

518

519 **Fig. 1.** *A-N*, optical photomicrographs showing the locations of 11 specimens of
520 five taxa of microfossils analyzed by SIMS (*B-D, F, G, I-N*) embedded in clouds of
521 flocculent organic matter permineralized in petrographic thin section 4 of 6/15/82-
522 1H of the ~3465 Ma Apex chert (*A*) and in its contained subrounded carbonaceous
523 clasts (*E, H*). *O-S*, optical photomicrographs of a similar clast (*O*) and filamentous
524 microfossils (*P-S*) in petrographic thin section 4 of 6/15/82-1B archived at
525 London's Natural History Museum (2). *T-Z*, three-dimensional (*T*) and two-
526 dimensional (*U-Z*) Raman images of the part of the specimen enclosed by the red
527 rectangle in (*S*). (*A*) Thin section 4 of 6/15/82-1H. (*B, C*) *Archaeoscillatoriopis*
528 *disciformis* Schopf 1993 (specimens #G and #F, respectively). (*D*) *Primaevifilum*

529 *amoenum* Schopf 1992 (specimen #H). (*E*) Small clast. (*F, G, K*) *P. minutum*
530 Schopf 1993 (small clast specimens #2 and #3, and clast specimen #9,
531 respectively). (*H*) Clast. (*I, J, L, M*) *P. delicatulum* Schopf 1992 (clast specimens
532 #11, #6, #4, and #5, respectively). (*N*) Unnamed unicell (clast specimen #12). (*O*)
533 A subrounded carbonaceous clast. (*P-S*) Organic clast-enclosed specimens of *P.*
534 *amoenum*, the arrows in (*P*) denoting their locations within the clast. (*T-Z*) Raman
535 images (acquired in a spectral window centered on the kerogen "G" band at ~1605
536 cm^{-1}) in which the three-dimensional image in (*T*) has been rotated to show the
537 cylindrical morphology of the filament and (*U-Z*) show two-dimensional images at
538 increasing depths though the specimen (*U*, 0.75μm; *V*, 1.5μm; *W*, 2.25 μm; *X*,
539 3.0μm; *Y*, 3.75μm; *Z*, 4.0μm) that document its box-like kerogenous cell walls
540 (arrows in *U*) and their enclosed cell lumina (arrows in *V*).
541
542 **Fig. 2.** Eleven specimens of five taxa of filamentous microfossils analyzed by
543 SIMS in petrographic thin section 4 of 6/15/82-1H of the ~3465 Ma Apex chert
544 shown in transmitted light photomicrographs (*A, C, E, G, I ,K, M ,O ,Q , S, U*) and
545 two-dimensional Raman images that document the distribution of kerogen (*B, D,*
546 *F, H, J, L, N, P, R, T, V*; blue, acquired in a spectral window centered on the
547 kerogen "G" band at ~1605 cm^{-1}). (*A-D*) *Archaeoscillatoriopis disciformis* Schopf
548 1993 (*A, B*, specimen #F; *C, D*, specimen #G). (*E-H*) *Primaevifilum delicatulum*

549 Schopf 1992 (*E, F*, clast specimen #4; *G, H,* clast specimen #5). (*I, J*) *P. amoenum*
550 Schopf 1992 (specimen #H). (*K-N*) *P. delicatulum* Schopf 1992 (*K, L,* clast
551 specimen #6; *M, N,* clast specimen #11). (*O-T*) *P. minutum* Schopf 1993 (*O, P*,
552 clast specimen #9; *Q, R,* small clast specimen #2; *S, T,* small clast specimen #3).
553 (*U, V*) Unnamed unicell (clast specimen #12).
554
555 **Fig. 3.** Paired images of pre-SIMS transmitted light photomicrographs (color) and
556 post-SIMS SEM images (black and white) of 11 specimens of five taxa of
557 microfossils analyzed for $\delta^{13}C$ in petrographic thin section 4 of 6/15/82-1H of the
558 ~3465 Ma Apex chert. (*A, B*) clast specimen #4; (*C, D*) clast specimens #5 and #6;
559 (*E, F*) clast specimen #9; (*G, H*) clast specimen #11; (*I, J*) clast specimen #12; (*K,*
560 *L*) specimen #F; (*M, N*) specimen #G (session-1); (*O, P*) specimen #G (session-2);
561 (*Q, R*) specimen #H; (*S, T*) small clast specimen #2; (*U, V*) small clast specimen
562 #3. White circles in the photomicrographs indicate the locations of the SIMS-
563 produced analytical pits. In the SEM images, (*J*) is a back-scattered electron
564 (BSE) image; all others are secondary electron (SE) images. These SEM images
565 were acquired in sections veneered with a thin (<~5-nm-thick) gold coat after
566 removal of a thicker Au-coat used during SIMS analyses and show the locations of
567 analyzed spots having high (≥3 Mcps/nA) and marginally accepted (3 to 1.5
568 Mcps/nA) ^{12}C-yields. Not shown are carbon-poor analytical pits and SIMS-

obtained $\delta^{13}C$ measurements considered not to be reliable. See *Supplementary Information* for additional analytical data. Scale bars represent 10 μm.

Table 1. SIMS-determined carbon isotope values measured for the five taxa of microfossils in thin section 4 of 6/15/82-1H of the ~3465 Ma Apex chert here discussed. For detailed summaries of the data, see *Supplementary Information*.

Taxon (*Specimen*)	**Figures**	**Number of Measurements**	**$\delta^{13}C$‰ VPDB**
Unnamed Unicell			
(Clast #12)	Figs. 1n; 2u v; 3i, j	1	-30.9
		(n = 1)	***Avg. -30.9***
Primaevifilum minutum			
(Clast #9)	Figs. 1k; 2o, p; 3e, f	1	-34.1*
(Small Clast #2)	Figs. 1f; 2q, r; 3s, t	1	-30.9
(Small Clast #3)	Figs. 1g; 2s, t; 3u, v	1	-29.8
		(n = 3)	***Avg. -31.6***
Primaevifilum delicatulum			
(Clast #4)	Figs. 1l; 2e, f; 3a, b	1	-32.7
(Clast #5)	Figs. 1m; 2g, h; 3c, d	1	-38.2
(Clast #6)	Figs. 1j; 2k, l; 3c, d	1	-36.9
(Clast #11)	Figs. 1i; 2m, n; 3g, h	1	-33.6
		(n = 4)	***Avg. -35.4***
Archaeoscillatoriopsis disciformis			
(Specimen #F)	Figs. 1c; 2a, b; 3k, l	1	-41.7
(Specimen #F)	Figs. 1c; 2a, b; 3k, l	1	-44.1**
(Specimen #G, Session-1)	Figs. 1b; 2c, d; 3m, n	1	-32.6*
(Specimen #G, Session-2)	Figs. 1b; 2c, d; 3m, n	1	-38.5***
		(n = 4)	***Avg. -39.2***
Primaevifilum amoenum			
(Specimen #H)	Figs. 1d; 2i, j; 3q, r	1	-39.4
		(n = 4)	***Avg. -39.4***

* Marginal ^{12}C-yield spots (see text).

** Repeat analysis.

*** Excluding high-$\delta^{13}C$ outlier (-9.7‰).

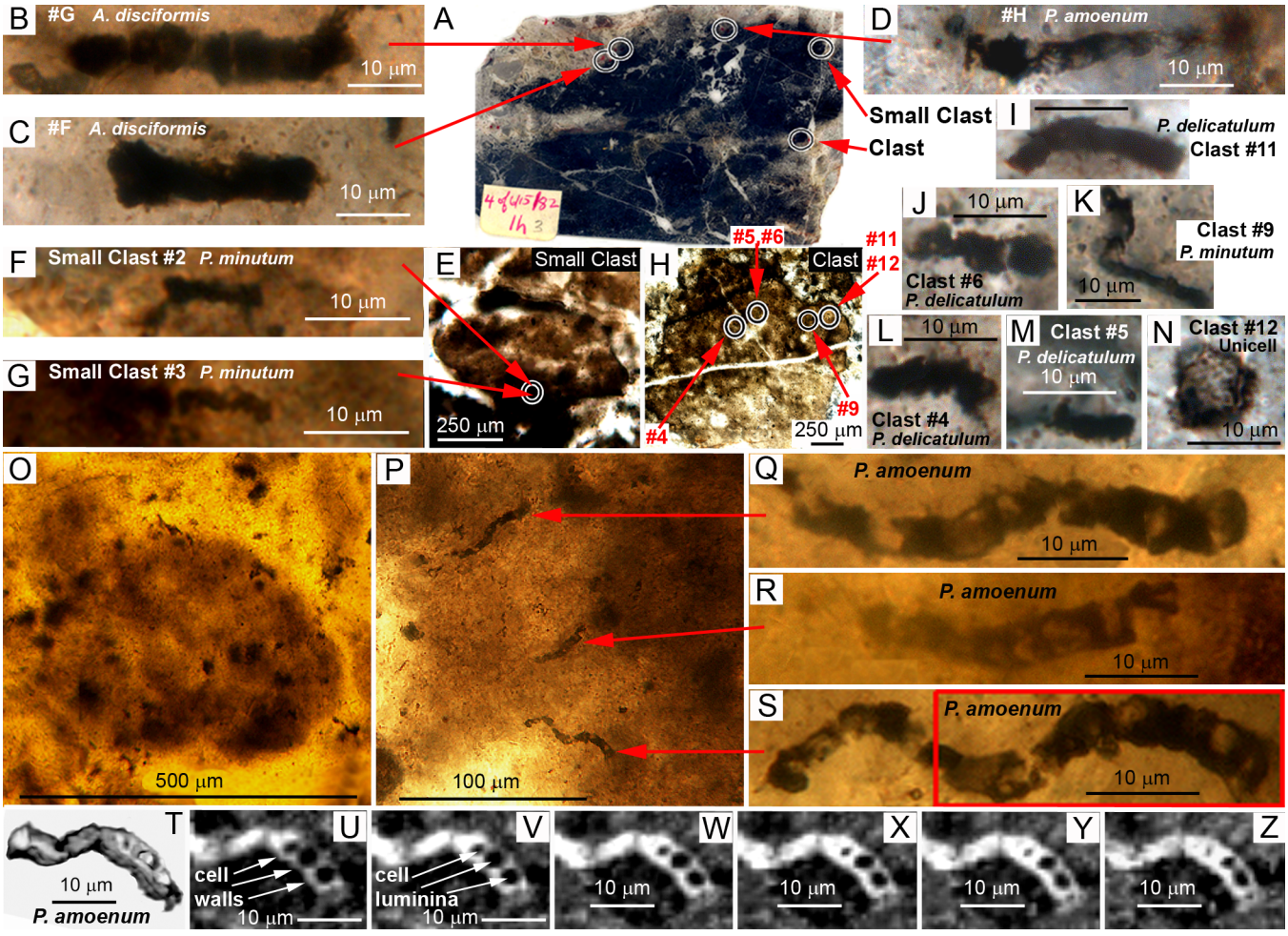
B #G A. disciformis
10 µm
C #F A. disciformis
10 µm
A
Small Clast
Clast
D #H P. amoenum
10 µm
I
P. delicatulum
Clast #11
J 10 µm
Clast #6
P. delicatulum
K
Clast #9
P. minutum
10 µm
F Small Clast #2 P. minutum
10 µm
G Small Clast #3 P. minutum
10 µm
E Small Clast
250 µm
H
#5,#6
#11
#12
Clast
#4
#9
250 µm
L 10 µm
Clast #4
P. delicatulum
M Clast #5
P. delicatulum
10 µm
N Clast #12
Unicell
10 µm
O
500 µm
P
100 µm
Q P. amoenum
10 µm
R P. amoenum
10 µm
S P. amoenum
10 µm
T
10 µm
P. amoenum
U
cell
walls
10 µm
V
cell
luminina
10 µm
W
10 µm
X
10 µm
Y
10 µm
Z
10 µm

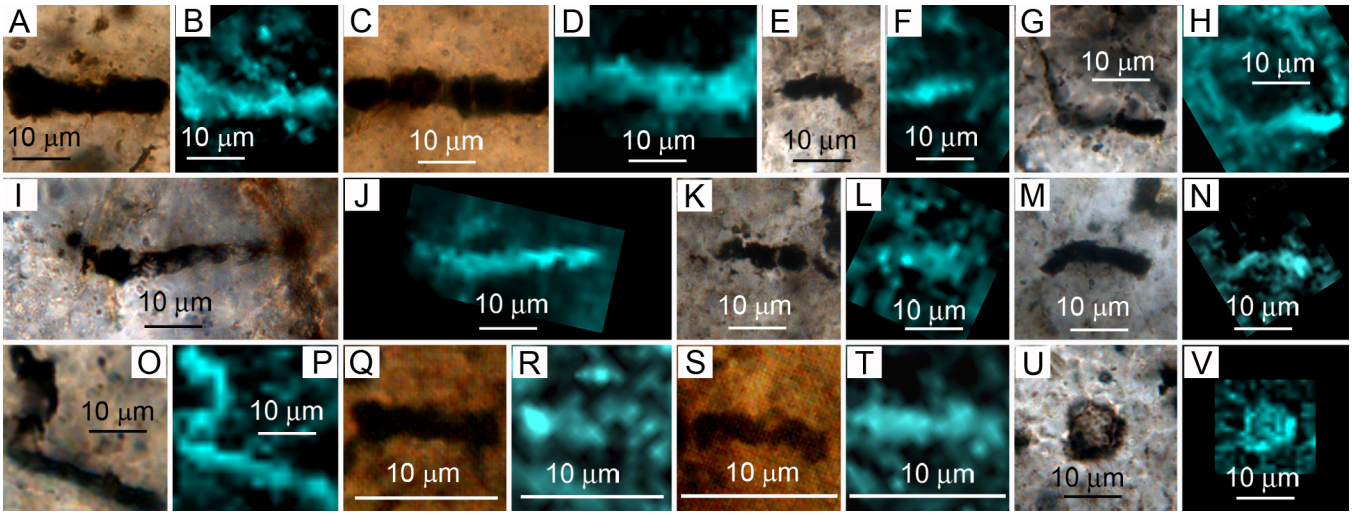
A
10 µm
B
10 µm
C
10 µm
D
10 µm
E
10 µm
F
10 µm
G
10 µm
H
10 µm
I
10 µm
J
10 µm
K
10 µm
L
10 µm
M
10 µm
N
10 µm
O
10 µm
P
10 µm
Q
10 µm
R
10 µm
S
10 µm
T
10 µm
U
10 µm
V
10 µm

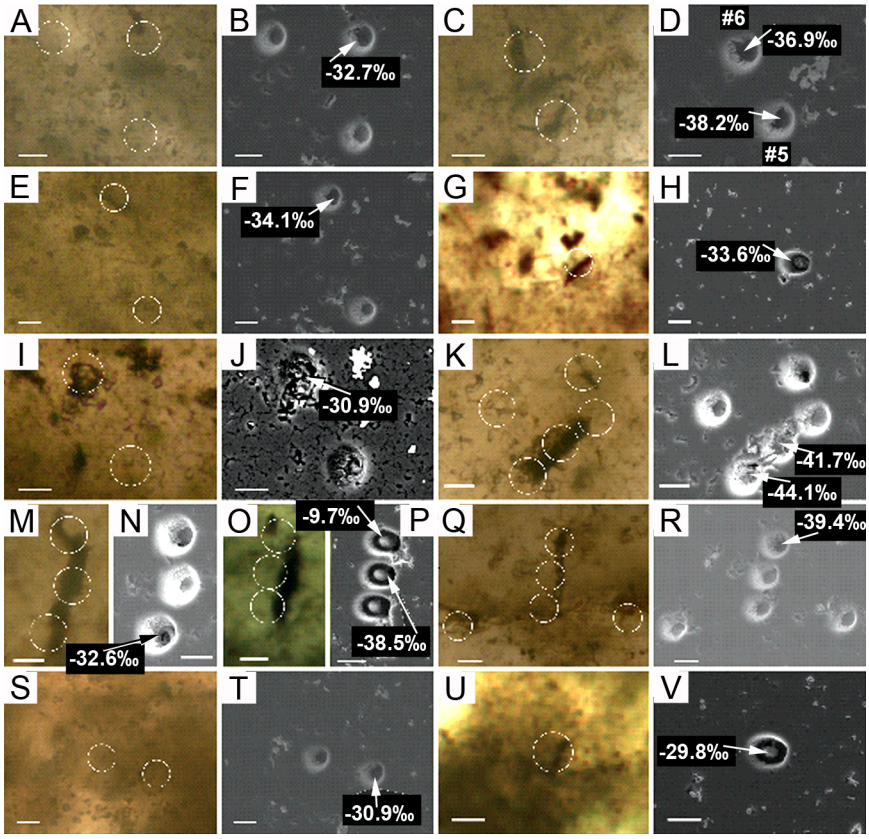
A
B
-32.7‰
C
D
#6
-36.9‰
-38.2‰
#5
E
F
-34.1‰
G
H
-33.6‰
I
J
-30.9‰
K
L
-41.7‰
-44.1‰
M
N
-32.6‰
O
-9.7‰
P
-38.5‰
Q
R
-39.4‰
S
T
-30.9‰
U
V
-29.8‰